Larval zebrafish respond to the alarm pheromone *Schreckstoff* by immobility and a change in brain state

Suresh Jesuthasan[1,2☯‡], Seetha Krishnan[3☯¤], Ruey-Kuang Cheng[1], Ajay Mathuru[2, 4, 5‡],

1 Lee Kong Chian School of Medicine, Nanyang Technological University Singapore, Singapore.
2 Institute of Molecular and Cell Biology, A*STAR, 61 Biopolis Drive, Singapore.
3 NUS Graduate School of Integrative Sciences and Engineering, National University of Singapore, Singapore
4 Yale-NUS College, 12 College Avenue West, Singapore.
5 Dept. of Physiology, Yong Loo Lin School of Medicine, National University of Singapore, Singapore.

☯These authors contributed equally to this work. ¤Current address - Biological Sciences Division, University of Chicago
‡Correspondence: ajay.mathuru@yale-nus.edu.sg; sureshj@ntu.edu.sg

Abstract

Danger signals elicit an immediate behavioural response as well as a prolonged increase in sensitivity to threats. We investigated the alarm response in larval zebrafish to identify neural circuits underlying such transitions. 5-7 day old larvae react to the alarm substance (*Schreckstoff*) by increased intervals between swim bouts and extended immobility. Calcium imaging indicates that olfactory sensory neurons innervating a lateral glomerulus detect the substance. Several telencephalic regions including the entopeduncular nucleus are also activated, with sustained activity outlasting stimulus delivery observable in the lateral habenula, posterior tuberculum, superior raphe, locus coeruleus, and periaqueductal gray. Consistent with the idea that these changes are related to an increased sensitivity to threats, larvae show increased dark avoidance after *Schreckstoff* removal. These results demonstrate that danger cues activate multiple brain circuits resulting in the expression of a continuum of defensive behaviors, some of which extend beyond stimulus detection.

Introduction

Behavioral and physiological changes in response to a danger signal increase the chances of survival in animals. These responses occur over multiple time-scales; immediate defensive behaviors that help evade predators [7] are coupled with long-term, system-wide changes to counter risk [1]. Regions of the vertebrate brain that process and execute immediate responses, such as the freeze or the flight responses [23, 30], and those mediating sustained responses [17, 56] have been identified in past studies [42]. Neuromodulators such as serotonin [12] and norepinephrine [26] have also been identified as having critical roles. However, a whole-brain view of the neural dynamics when transitions in central states [47] occur in an animal in response to a threat is lacking.

Here, we explored the use of larval zebrafish, where *in vivo* brain-wide imaging of neural activity can be conducted with relative ease [14, 24], to examine neural circuits

and their dynamics during the transition in brain state in response to danger. As a danger cue, we turned to alarm substances (or *Schreckstoff*). These are released upon physical injury to an individual and elicit a striking *Schreckreaktion*, or an alarm response, in the entire shoal [16,25,36,48]. In general, the detection of such a cue results in an immediate change in locomotion [28,49]. In zebrafish, in addition, other changes such as an increase in anxiety-like behaviors remain even after the removal of the cue [32,38], making it a good system to examine the steps in changes in central states.

Whether early zebrafish larvae (5-7 day old) ideally suited for whole-brain imaging show a *Shreckreaktion* has been debated. One study examined the ontogeny of the response in zebrafish in detail by quantifying behavioral parameters associated with alarm in adults. This study reported that the earliest responses can be seen only around day 42 days post fertilization [53]. This mirrors reports in fathead minnows that observable responses occur only after 48-57 days post-hatching [13]. These observations are consistent with older studies that tie the initial onset of typical adult-like alarm response with the development of shoaling behavior and mixed feeding as larvae reach a juvenile stage (in most species between 28-40 days post fertilization [21]). However, although adult-like responses may appear only later in ontogeny, it is possible that larvae are capable of sensing and responding to the alarm cue in a different manner [22,35].

As larval and adult differences in kinematics, and sensitivity of as much as a million-fold have been documented in many species [21], we explored the use of a chamber size-matched to the larva that mimics the adult behavioral setup we had used in the past to quantify the behavior of a solitary animal [37]. We complemented our behavioral studies with neural activity imaging of transgenic lines expressing GCaMP6f. Both our behavioral and imaging experiments suggest that larval zebrafish show a dynamic response to *Schreckstoff* even at this early age, characterized by an acute change in behavior followed by a change in wariness. These are correlated with transient activation of olfactory sensory neurons innervating a lateral glomerulus and sustained activity in many regions of the midbrain.

Materials and Methods

Ethics statement

All experiments were carried out under guidelines approved by the IACUC of A*STAR (number 181408).

Experimental methods

Are described in detail in extended supplementary data.

Results

Quantifying larval swimming behavior in a vertical column.

We used a simple assay chamber that allowed observation of larval swimming behavior in a 50 mm vertical column (Supplementary Figure 1; [33];see methods). We first characterized and identified quantifiable parameters associated with normal swimming of 5-7 dpf larvae in this type of chamber over a period of 30 minutes. As described in the past for larvae of an equivalent age [11], larvae swam in short bouts (Fig 1A, 1B). Larvae explored the entire chamber but preferred to stay in the top quarter of the chamber reaching an average depth of about 14 mm (Figure 1C, Supplementary Figure

1). The average duration of each swimming bout was 246.40 ms (95% CI [245.59 ms, 247.21 ms]) and each inter-bout interval lasted 173.11 ms (95% CI [169.05 ms, 177.18 ms]). The histogram of swimming speed plotted per second (Figure 1D) showed a bimodal distribution with one peak in the 0 mm/sec bin reflecting the distribution of time spent in the two modes, swimming, and inter-bout intervals. We examined if the swimming behavior of larvae changed as a function of the time spent in the assay chamber. We examined 10-minute windows, on either side of the intended stimulus delivery time (calling them Pre and Post; arrow Figure 1F). We also included a second 10-minute window after the first post-stimulus delivery period (10'-20' Post) to examine delayed responses if any. No differences in the distance swam (Figure 1F) or in the inter-bout intervals (Figure 1E) could be detected. Therefore, the swimming behavior of the zebrafish larvae did not show any noticeable change in the 30 minute observation period of the experiment.

Larval zebrafish display a startle response to stimulus delivery

Change in illumination [6], acoustic, or mechanical disturbances [34] can startle zebrafish larvae. We reasoned that a liquid stimulus delivery into the observation chamber however gently performed will disturb the water column and startle the larvae. To test this, we compared the behavior of larvae when tank water was delivered into the chamber as a control stimulus (Supplementary Figure 2). The brief stimulus delivery period (5 seconds) was excluded from the analysis. Histogram of speed distribution reflected the observations in Figure 1 that there were no differences between the three time-bins in the no stimulus delivery condition (Spplementary Figure 2).

Control (tank water) delivery however changed speed distribution (Supplementary Figure 2A). Larvae increase the time spent motionless (Supplementary Figure 2B). The change is reflected in increased inter-bout interval as the average duration of a swimming period remains unchanged at 244.99 ms (95% CI [243.58 ms, 246.40 ms]), while the average inter-bout interval increased from 171.76 ms (95% CI [168.36 ms, 175.15 ms]) to 190.89 ms (95% CI [182.06 ms, 199.71 ms]; Pre with Post, $p = 0.001$, Student's t-test).

Few individuals can contribute disproportionately to an average readout, such as the one quantified above. To examine if this could be the case here, we compared the number of individuals that showed higher than average immobility in the two conditions. In the no stimulus condition, larvae spent approximately 24 seconds or 4.18 % of the 10-minute window being immobile (95% CI [1.72%, 6.64%], standard deviation = 7.60%; Supplementary Figure 2B). In the Pre time-bin, only 10% of individuals (4 of 40; Supplementary Figure 2C) were immobile for periods longer than the average by 1 SD or more (i.e. for 11.78% or longer of the 10-minute window). This percentage was unchanged in the Post and the 10'-20'Post time-bins (Supplementary Figure 2C and 2D). In the stimulus delivery condition this percentage increased to approximately 20% of individuals (9 out of 40; Supplementary Figure 2C and 2D). Therefore, a greater number of individuals were immobile for longer periods after the mechanical disturbance caused by control stimulus delivery. The inter-bout interval increased upon stimulus delivery, but the average swimming period in a bout did not change.

Larval zebrafish respond to adult-derived *Schreckstoff*

Given that the stimulus delivery itself can elicit a detectable change in the behavior of larvae, we examined larval responses to 3 concentrations (low, medium, and high) of *Schreckstoff*. We reasoned that if larvae respond to the alarm substance then it may show a concentration dependence, while a response purely to the mechanical disturbance produced by the process of *Schreckstoff* delivery will be independent of concentration. The histogram of speed distribution showed a marked change after stimulus delivery in

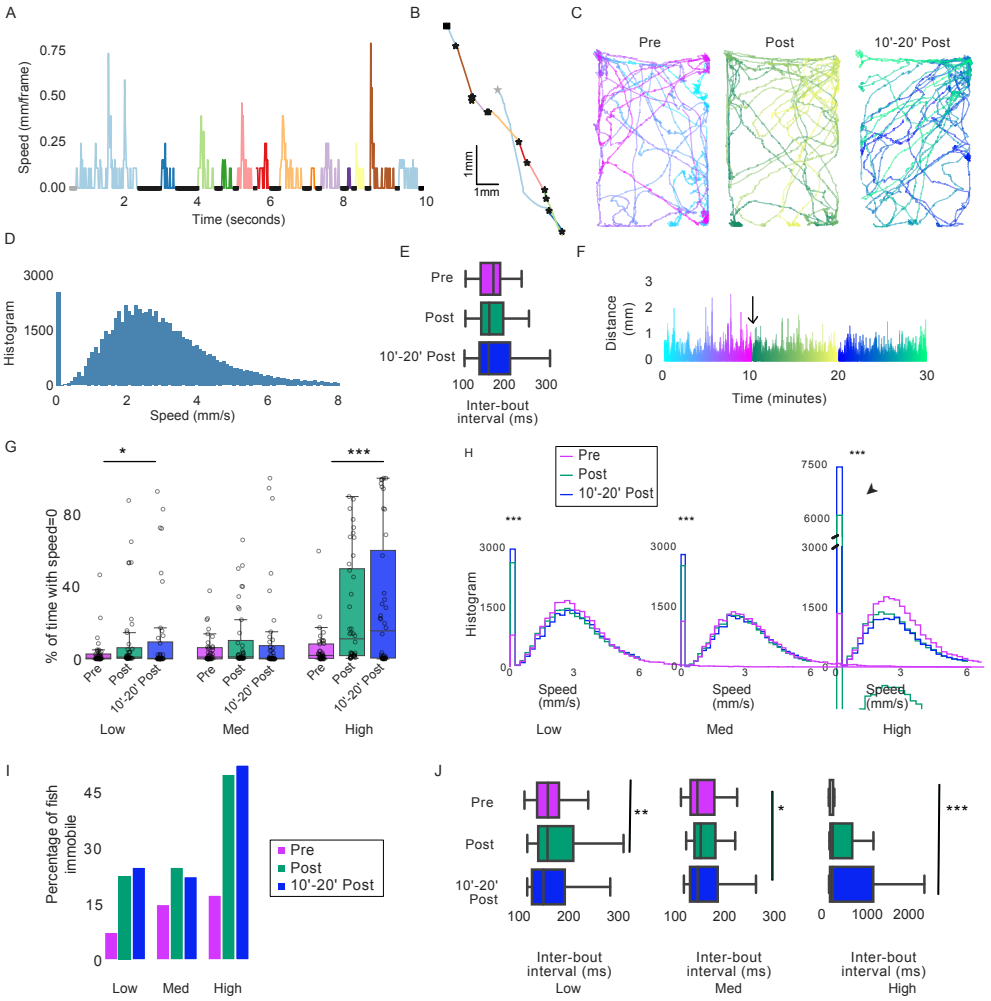

Figure 1. Quantification of larval behavior to *Schreckstoff* in a vertical column.. (A) Trace shows instantaneous speed over a few seconds in one larva. Swimming periods are interspersed with periods of speed = 0 (Black dots). (B) The trajectory of the same animal. Grey star indicates time = 0. Bout trajectories are color coded to panel A and black stars indicate start of a swim bout. Bouts vary in length and distance moved. Representative (C) tracks and (F) distance swam (in mm) color-coded over three 10 minute bins - Pre, Post and $10' - 20'$ Post. Stimuli, if delivered were delivered at the time indicated by the arrow in F. (D) Histogram of the speed (mm/sec) over the entire period shows the binomial distribution due to time spent in swimming bouts interspersed with inter-bout intervals of 0 speed. (E) Inter-bout intervals in the three time-bins do not change significantly over time. (G) Percentage of fish with speed = 0 mm/sec for $> = 1$ SD than the average immobility time in the Pre time-bin of the no stimulus condition, (H) Histograms of speed distribution (in mm/s), (I) Boxplots of the percentage of time spent motionless and (J) Inter-bout intervals in the three time-bins in three time-bins for the conditions to three concentrations of *Schreckstoff* (low, medium and high) in the Pre, Post, and 10'-20' Post time-bins. Circles represent the individual fish response. Change is most notable in the high condition * indicate p values < 0.05, ** < 0.01, and *** indicate < 0.0001 in paired t-tests or KS test. Exact p values are given in the text; n = 40/condition

both low (Figure 1H; Low, Pre with 10' Post: p=0.0002; Pre with 10'-20' Post: p=0.00004, KS Test) and medium *Schreckstoff* conditions (Figure 1H; Med, Pre with 10' Post: p=0.0002; Pre with 10'-20' Post: p=0.0008, KS Test). The total time spent immobile showed a modest increase (Figure 1G). The inter-bout interval also increased after stimulus delivery from 160.38 ms (95% CI [155.52 ms, 165.23 ms]) to 198.29 ms (95% CI [180.32 ms, 216.26 ms]) in the case of low (Figure 1J; p <0.0001, Student's t-test), and from 160.31 ms (95% CI [152.62 ms, 168.00 ms]) to 179.70 ms (95% CI [166.40 ms, 192.97 ms]) in the case of the medium concentration (Figure 1J; p = 0.012, Student's t-test). These changes, however, were not unlike those observed for the control delivery condition described above, and a similar number of individuals (approximately 20%) showed a change in the behavior (Supplementary Figure 2).

The larval response to the highest concentration of *Schreckstoff*, on the other hand, was much more striking (Supplementary Figure 3; Supplementary Movie 1). The speed distribution histogram showed a substantial and prolonged increase in immobility (Figure 1H, SS high; Pre with 10' Post: p=6.8*10-8; Pre with 10'-20' Post: p=1.2*10-9, KS Test; Supplementary Figure 3). 50% of the fish (20/40) showed such a response a(Figure 1I). The duration of swimming bouts did not change much from 239.33 ms (95% CI [238.02 ms, 240.64 ms]) to 230.25 ms (95% CI [228.83 ms, 231.67 ms]), but the inter-bout interval (Figure 1J, p <0.0001, Student's t-test) increased from 188.53 ms (95% CI [182.85 ms, 194.22 ms]) to 320.58 ms (95% CI [273.76 ms, 367.40 ms]).

Adult zebrafish show a diving response to *Schreckstoff* [37]. Supplementary Figure 5 shows the location and duration of the immobility of all the animals tested after exposure to the control stimulus (tank water) or to the highest concentration of *Schreckstoff*. The diameter of the circles is proportional to the duration of immobility as a percentage of that time-bin (10 minutes). Larvae become immobile in different parts of the chamber. Therefore, larvae show a qualitatively similar response to control stimulus delivery at low concentrations of *Schreckstoff*, but quantitatively different response when a high concentration was delivered. Greater number of fish show an immobility response. Therefore, 5-7 dpf larvae can sense and respond to adult-derived *Schreckstoff*.

A lateral glomerulus in the olfactory bulb of larval zebrafish senses adult-derived *Schreckstoff*

Next, we examined the neural activity in the larvae. We first imaged the olfactory bulbs of 5-7 day old *Tg(gng8:GAL4, UAS:GCaMP6s)* larvae where a small subset of olfactory microvillus sensory neurons express GCaMP6s [44], and delivered *Schreckstoff* as described previously [15, 37]. A response to *Schreckstoff* was observed in the glomerular termini of gng8-expressing neurons (Figure 2 A-C). In the zebrafish, the position of large glomeruli is invariant as they are located in the same relative organization across individuals [9]. The developmental patterns of such large glomeruli can be traced from 72 hpf or 3 dpf onwards and reliably mapped even if the smaller glomeruli change in number and location in an experience dependent manner [10]. These are identifiable as in addition to the anatomical location in the X, Y and Z planes, the glomerular map can also be consistently derived on the basis of immunoreactivity to markers like calretinin and $G\alpha s/olf$ [10].

We stained *Tg(gng8:GAL4, UAS:GCaMP6s)* larvae (Figure 2D-G) with anti-calretinin (Fig 2H-J) and anti- $G\alpha s/olf$ (Figure 2K-P) antibodies. Antibody staining show that the *Schreckstoff* responsive glomerulus is calretinin positive but is not labeled by the anti- $G\alpha s/olf$ antibody. Therefore, based on the nomenclature proposed in [9], the *Schreckstoff* responsive glomerulus is located in the lateral glomerular cluster, most likely LG_4, and is innervated by GnG8 positive neurons.

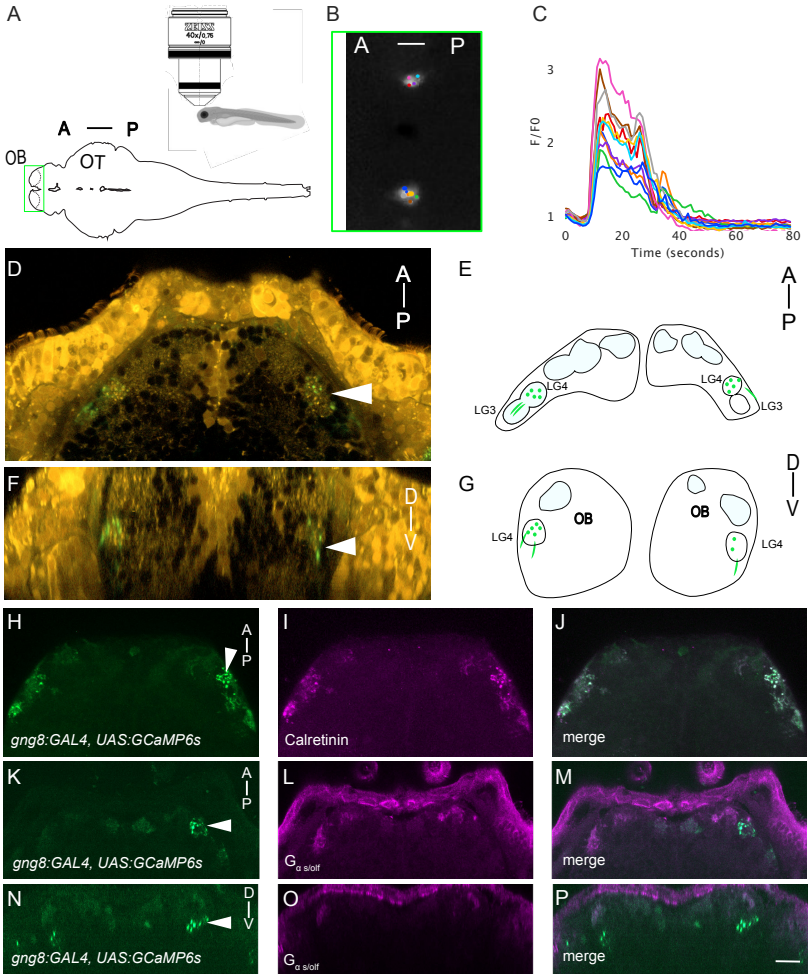

Figure 2. Larval OSNs targeting a lateral glomerulus respond to *Schreckstoff*. A) Schematic of the imaging setup for calcium imaging B) One frame from a F/F0 series, where fluorescence increase was maximal. C) Plot of 11 terminals, showing a rise in intracellular calcium in response to adult skin extract, which was delivered from 5 - 25 seconds. *Tg(gng8:GAL4, UAS:GCaMP6f)* fish, labeled with $4-Di-2-ASP$ (shown in orange), which enables visualization of glomeruli. D) Dorsal view F) Frontal view through the stack. E) and G) show lateral glomerulus schematic based on D and F respectively. Labelled neurons (green) terminate in a lateral glomerulus. H) *Tg(gng8:GAL4, UAS:GCaMP6f)* stained with I) anti-calretinin and J) merge shows that transgenic neurons are Calretinin positive. K and N) *Tg(gng8:GAL4, UAS:GCaMP6f)* larvae stained with anti- $G\alpha s/olf$ antibody visualized in L) dorsal and O) frontal views show no overlap in the O), and P) merge. A - Anterior and D - Dorsal is to the top in all images, P - Posterior, V - Ventral. Scale bar = 10 μm.

Brain-wide responses to adult-derived *Schreckstoff*

Neurons from the larval olfactory bulb project to several regions in the forebrain, including the posterior telencephalon (Dp), ventral telencephalon (Vi and Vv) and dorsal right habenula [39]. To determine whether these regions show a change in activity as a result of exposure to the alarm substance, we recorded from the forebrains of 5-7 day old fish with broad expression of nuclear-localized GCaMP6f (*(Tg(elavl3:h2b-GCaMP6f)*), using a two-photon resonant scanning microscopy with

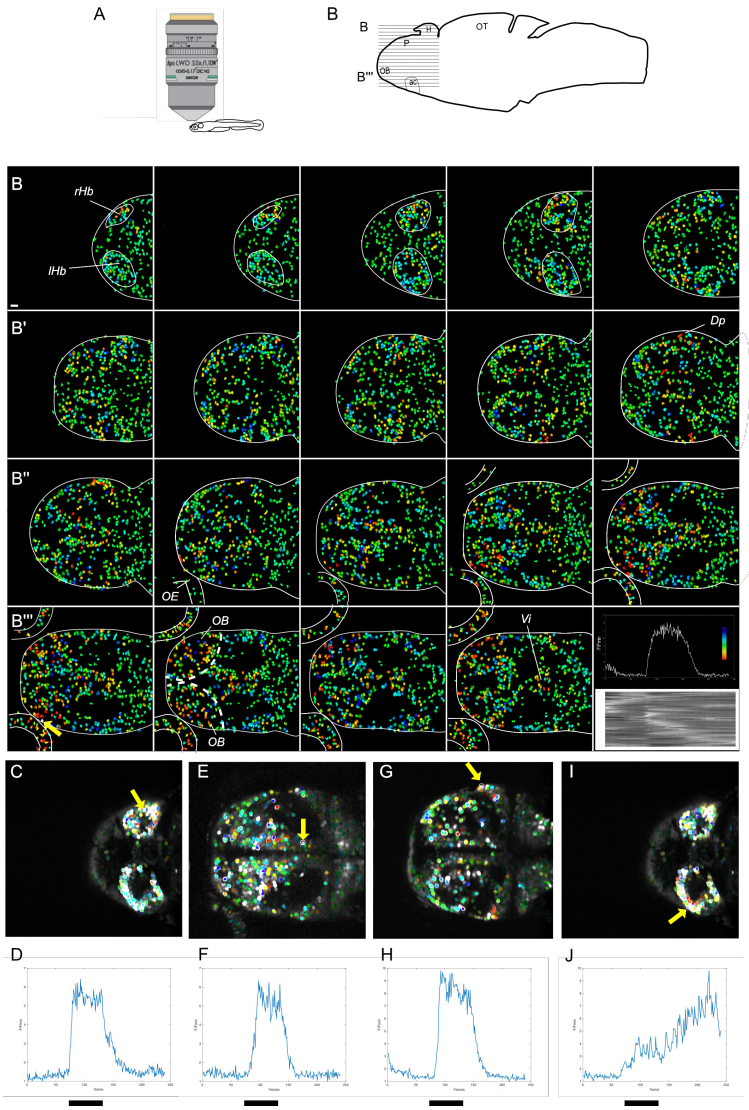

Figure 3. Forebrain responses to *Schreckstoff*. A) Schematic of the imaging setup for calcium imaging. B) Activity in nineteen focal planes (B' to B''') of the forebrain of a 7 day-old zebrafish, from dorsal (top left) to ventral (bottom row). Cells are color coded according to correlation with the indicated cell (bottom left panel), which is in the lateral olfactory bulb. The relative change in fluorescence of this cell is shown in the bottom right. The wedge shows the lookup table employed in mapping correlation. The raster plot shows raw fluorescence in > 7000 cells across all planes. C-J). Three different focal planes from the image in panel B, overlaid on a mean image of the fluorescence t-stack. These show three major targets of the olfactory bulb, which are Dp (C), Vv (E) and the habenula (G, I). Relative fluorescence change of the cell indicated indicated by the yellow arrow is shown in the plot below the corresponding image. The black bars indicate the stimulus. rHb - right habenula, lHb - left habenula, Dp - posterior telencephalon, Vi - intermediate ventral telencephalic nucleus, OE - olfactory epithelium, OB - olfactory bulb.

piezo focusing to allow volume imaging (Figure 3 A, B). Correlated change in the activity was seen in the olfactory epithelium, olfactory bulb, Dp, Vi and habenula in all

fish imaged (Figure 3 C-H; n = 7 fish). In addition to this correlated activity, we also observed a persistent increase in the activity in a subset of neurons in the lateral habenula of all fish (Figure 3 I, J; Supplementary Figure 6).

The lateral habenula receives direct input from the entopeduncular nucleus [3, 51], which is homologous to the internal segment of the globus pallidus in mammals. Imaging of larval fish expressing a fluorescent label in the entopeduncular nucleus *Tg(elavl3:h2b-GCaMP6f),etSqKR11* indicates that *Schreckstoff* elicits activity in this nucleus (Supplementary Figure 7). A mixture of activity patterns was seen, including activity during and after the stimulus (Supplementary Figure 6). Thus, in addition to areas predicted by direct connectivity with the olfactory bulb, the alarm substance influences a number of other areas within the forebrain, including a structure involved in processing negatively valenced stimuli [31].

The habenula provides a pathway from the forebrain to midbrain neurons. To determine if the habenular activity is accompanied by a change in midbrain activity, calcium imaging was carried out across a larger region of the brain (Figure 4A, n = 6 fish). Activity after exposure to the stimulus was distinct from activity before exposure (Figure 4B), indicating a change in brain state. In contrast to the olfactory bulb and telencephalon (Figure 4C-E), where there was a transient increase in activity that correlated with delivery of *Schreckstoff*, neurons in the midbrain tegmentum, superior raphe, posterior tuberculum and locus coeruleus showed persistent activity Figure (4F-H). These regions were identified based on anatomical landmarks as described in the methods. Thus, transient exposure to skin extract elicits an extended neuronal response in the diencephalon and midbrain.

Larval zebrafish behavior changes after exposure to the alarm substance

Adult zebrafish show an increase in anxiety-like behaviors after exposure to the alarm substance, as observable by a change in their responses in the light/dark assay [38]. In such a novel environment adult zebrafish display scototaxis, that is, a preference for the dark side of the chamber. This natural response is further enhanced after exposure to *Schreckstoff* [38]. Zebrafish larvae, on the other hand, are known to display scotophobia or dark avoidance in such an assay [50].

To test whether scotophobia in larvae is also increased, indicative of lasting anxiogenic effects of transient exposure to *Schreckstoff*, we placed them in assay tanks that offered a choice between light and dark backgrounds after washing off the alarm substance. 7 dpf larvae showed an increase in scotophobia compared to control larvae exposed only to the tank water spending less time in the dark side of the tank (Figure 5A; mean difference = -5.49 [95CI = -9.39, -1.36], Cohen's d = 0.6 Student's t-test p = 0.01) and making fewer entries into the dark side (Figure 5B; mean difference = -0.9 [95CI = -0.43, -1.33], Cohen's d = 0.95 Student's t-test p = 0.0001). Alarmed larvae (n=40) are more risk averse and are more cautious compared to controls as they enter the dark side later. This is also reflected at a population level by the shallow slope of a quadratic function fit for the time to first entry to dark (Figure 5C). Therefore, zebrafish larvae exhibit anxiety-like behaviors after transient exposure to an alarm cue and remain cautious indicative of a changed central brain state.

Discussion

In this study, we examined the alarm response in early larval zebrafish to study brain state transitions during danger. Behavioral studies were conducted in a size proportionate arena, at an age when free-swimming and hunting begins. We find that

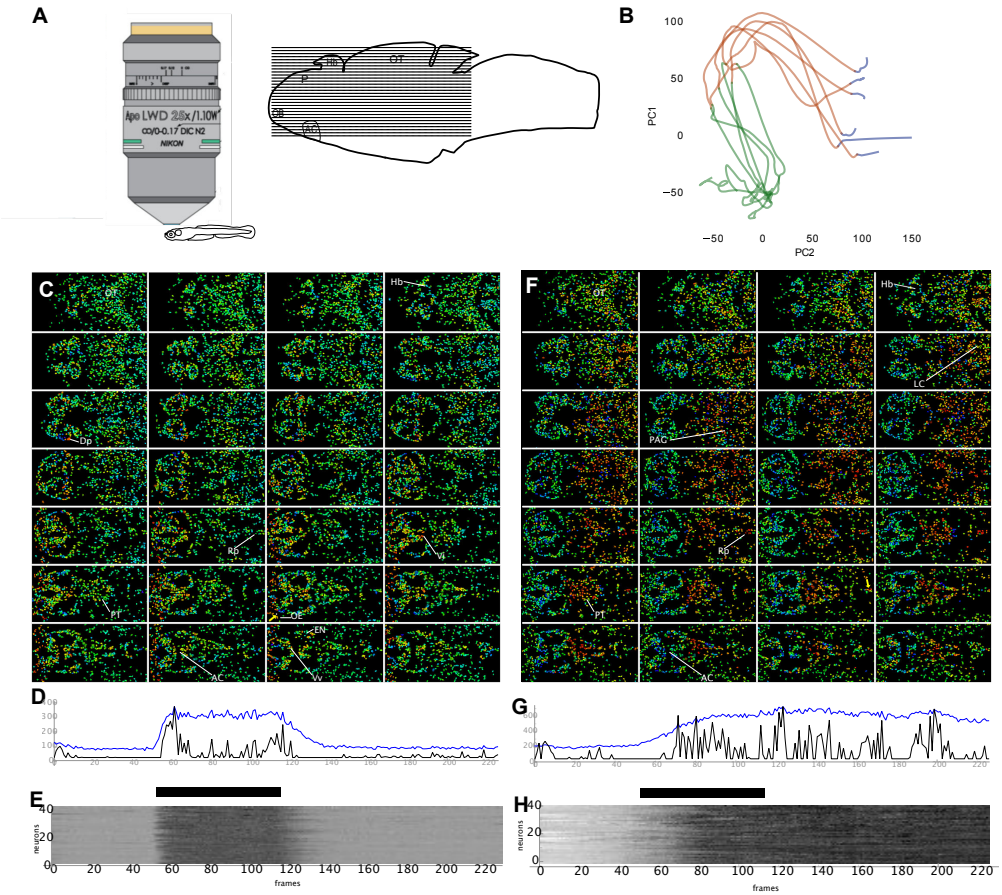

Figure 4. Contrasting dynamics in the forebrain and midbrain following *Schreckstoff* exposure. A) Schematic diagram of imaging set-up. The horizontal lines indicate the approximate location of the region imaged. 28 planes were recorded, 5 μm apart. B) Trajectory of neural activity across the forebrain and midbrain of six fish, shown in two-dimensional state space. The colours indicate activity before (blue), during (red) and after (green) *Schreckstoff* delivery. C - H) Response in one 7 dpf fish to a pulse of *Schreckstoff*. Cells are colour-coded according to correlation coefficient with the indicated cell (yellow arrow), which is in the olfactory epithelium in panel C and in the raphe in panel F. D), G) The raw fluorescence (blue) and deconvolved trace (black) of the cell in panels C and F respectively. E), H). Heatmap of response in 40 cells that are most correlated with the cell indicated in panels C and F respectively. OT: optic tectum, AC: anterior commissure, Hb: habenula, Dp: Posterior telencephalon, Rp: superior raphe, LC: locus coeruleus, PAG: periaqueductal gray, EN: entopeduncular nucleus, Vi: intermediate ventral telencephalic nucleus.

larvae show a quantifiable change in locomotion in response to *Schreckstoff*. Unlike adults with complex kinematics, larval fish only show an increase in immobility and an increase in the inter-bout intervals. Further, only a subset of larvae show a noticeable vertical displacement towards the bottom of the tank, in contrast to the downward movement prominent in adults. A relatively subtle response can therefore be easily missed, likely contributing to the inconsistent reports in the past. The reason for the differences between adults and larvae could be multifold. One possibility is the immaturity of the neuromuscular apparatus and/or the neural circuitry needed to

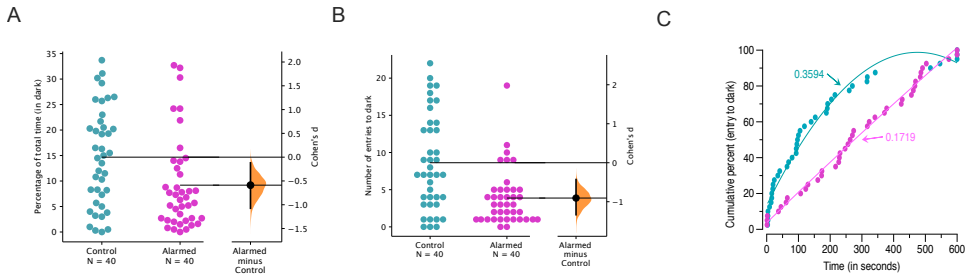

Figure 5. Effect of *Schreckstoff* on dark avoidance of larval zebrafish. A) The percentage of total time (of 10 minutes) spent in the dark, or B) the number of entries to the dark side and C) shows the time taken for cumulative percentage for the first entry to the dark side to reach 100% for control (teal) or alarmed (magenta) larvae. For A and B, Both groups are plotted on the left axes; the mean difference is plotted on floating axes on the right as a 5000 bootstrap sample distribution. The mean difference values are given in the text and are depicted as a dot; the 95% confidence interval is indicated by the ends of the vertical error bar.

execute adult-like erratic swimming at this stage of development [40], although escape responses requiring brief periods of powered swimming are well documented [11, 34, 52]. Another possibility is that the differences in behavior improves survival at each stage [41]. Regardless, larvae display a quantitatively discernible response to the alarm substance from an early age.

The lexicon describing "emotions" and its applicability to animals is debated extensively. We favor the simpler framework of operationalizing the functional and adaptive properties of observable behaviors in animals [2, 4]. In this framework, internal states are expected to be triggered by specific external stimuli and manifest as observable changes, such as defensive behaviors. Fear in this context has been defined as an acute response to a danger cue [45], while anxiety is the response when the threat is uncertain. This can occur when a danger cue is no longer detectable [27]. Upon smelling a cat, for example, a rat will freeze in place, or escape depending on the imminence of the danger [8]. Rodents have been shown to display increased "wariness" described as anxiety-like behaviors subsequently [1]. Similarly, adult zebrafish become vigilant and display more anxiety-like behaviors after the removal of the alarm cue [32, 38]. Consistent with these and other studies [22, 35], we find that 5-7 day old zebrafish respond to the alarm pheromone both with an immediate, and an extended response.

Volumetric two-photon calcium imaging of 5-7 day old larvae revealed that at least some components of the neural circuitry required to mediate such changes after predator detection develop early. Previous reports indicated that at least two glomeruli in the lateral and medial olfactory bulb regions respond to the alarm substance [19, 37]. Present results indicate that the glomerulus in the lateral bulb (LG) is innervated by microvillous olfactory sensory neurons [15]. The LG cluster consists of 2 identifiable large glomeruli, LG_3 and LG_4 from 3 dpf onwards in the classification proposed by Braubach et. al [10]. Among them, LG_4 was reported to be the only glomerulus in the LG that is unresponsive to amino acids [10]. Combining this with our observations suggests that the glomerulus activated by*Schreckstoff* in this cluster is likely to be LG_4. Future experiments where the activity of this glomerulus is controlled in an optogenetic or a chemogenetic manner will be required to validate this hypothesis.

Among the known targets, correlated activity downstream of the olfactory bulb was seen in the lateral region of the pallium and in the ventral telencephalon in our experiments. The former likely includes Dp (homolog of olfactory cortex [24]) and Dlv (homolog of the hippocampus [24]), while the latter likely includes the intermediate

nucleus of the ventral telencephalon, which receives input from the olfactory bulb and has been proposed to be homologous to the medial amygdala of mouse [5]. Not all targets of the olfactory bulb showed such a response. Activity detected in Vv, which is located rostral to the anterior commissure [55] and proposed to be the homolog of the mammalian septal formation [24] were not correlated. The posterior tuberculum, another direct target of the olfactory bulb [39] showed even less correlated activity but was activated in a sustained manner.

In contrast, several midbrain regions showed an extended increase in the activity after stimulus delivery. One of these is the superior raphe, which contains serotonergic neurons. One interpretation of this observation is that sustained activity in the raphe leads to persistent serotonin release mediating subsequent behavioral changes. This interpretation is consistent with experiments in adult zebrafish, where exposure to the alarm substance leads to an increase in extracellular serotonin [38]. A potential circuit that could mediate this increase in raphe activity is an excitatory input from the lateral habenula where a subset of neurons was activated in all fish imaged in our recordings. The lateral habenula has been shown to drive the activity of serotonergic neurons in the raphe [3], and lesioning of the lateral habenula blocks the response to *Schreckstoff* in adults [43]. The lateral habenula in turn, is known to receive input from the entopeduncular nucleus [3, 51] which was also activated during and after stimulus delivery in our recordings. It is unclear at this point what drives activity in the entopeduncular nucleus after stimulus removal, but the raphe itself is a potential source [3], creating a feed-forward loop. However, the possibility that local circuits mediate this activity cannot be excluded.

In addition to the raphe, sustained activity was seen in several other brain regions. Among these, activity in the locus coeruleus is consistent with increased norepinephrine reported in adults following exposure to *Schreckstoff* [38]. In the midbrain tegmentum, activity was detected in a region that is proposed to be the periaqueductal gray, based on the expression of *relaxin3a* and proenkephalin-like [20]. The significance of sustained activity in posterior tuberculum, which contains dopaminergic neurons [18, 54], is unclear. The nucleus in basal vertebrates is proposed to send both ascending and descending projections that disinhibit the downstream targets to initiate locomotion [46]. Further investigations are needed to dissect the relationship between the activity profile of the posterior tuberculum evoked by the alarm substance and the larval behavior reported here. Notwithstanding the future direction of studies, the observation that transient exposure to *Schreckstoff* causes extended activity in multiple nuclei suggests a model in which the transition to predator detection dependent anxiety involves multiple neuromodulators. This underscores the limitation of treating anxiety disorders with single compounds, assuming that subcortical circuit elements in related processes are shared across vertebrates.

Our results also raise a number of questions. Although calcium imaging identified numerous brain regions that change in activity it is unclear, for example, the mechanism that sustains persistent activity in midbrain nuclei in the absence of an external trigger. The temporal dynamics of potential feedback and feed-forward connections between different regions are difficult to infer at the current resolution. Connectome projects [29] and functional mapping could begin addressing such questions in the future. A combination of approaches that combines behavioral studies, whole-brain imaging, and neuroanatomical mapping to address these points has the potential to provide an unprecedented complete map of the neural circuits involved in a tractable system. With the use of molecular manipulation, the alarm response of larval zebrafish has the potential to serve as a powerful paradigm to understand the molecular and neural bases of fear and anxiety in a vertebrate.

Conclusion

Larval zebrafish can sense *Schreckstoff*. Most larvae (approximately 50%) show an immediate change in swimming behavior. Whole-brain imaging reveals a change in the brain state upon the perception of the alarm cue in the form of sustained activity in many mid-brain neuromodulator releasing regions. The larvae become vigilant after a brief exposure to the threatening cue, and transition to displaying defensive behaviors for an extended period even after the cue indicating danger is removed. Our study suggests that defensive behaviors operate over a continuum and involve multiple brain circuits.

References

1. R. E. Adamec and T. Shallow. Lasting effects on rodent anxiety of a single exposure to a cat. *Physiol. Behav.*, 54(1):101–109, July 1993.

2. R. Adolphs and D. J. Anderson. *The Neuroscience of Emotion: A New Synthesis*. Princeton University Press, June 2018.

3. R. Amo, F. Fredes, M. Kinoshita, R. Aoki, H. Aizawa, M. Agetsuma, T. Aoki, T. Shiraki, H. Kakinuma, M. Matsuda, M. Yamazaki, M. Takahoko, T. Tsuboi, S.-I. Higashijima, N. Miyasaka, T. Koide, Y. Yabuki, Y. Yoshihara, T. Fukai, and H. Okamoto. The habenulo-raphe serotonergic circuit encodes an aversive expectation value essential for adaptive active avoidance of danger. *Neuron*, 84(5):1034–1048, Dec. 2014.

4. D. J. Anderson and R. Adolphs. A framework for studying emotions across species. *Cell*, 157(1):187–200, Mar. 2014.

5. D. Biechl, K. Tietje, S. Ryu, B. Grothe, G. Gerlach, and M. F. Wullimann. Identification of accessory olfactory system and medial amygdala in the zebrafish, 2017.

6. B. H. Bishop, N. Spence-Chorman, and E. Gahtan. Three-dimensional motion tracking reveals a diving component to visual and auditory escape swims in zebrafish larvae. *J. Exp. Biol.*, 219(Pt 24):3981–3987, Dec. 2016.

7. D. C. Blanchard, E. B. Defensor, and R. J. Blanchard. Fear, anxiety, and defensive behaviors in animals, 2010.

8. R. J. Blanchard, M. A. Hebert, P. F. Ferrari, P. Palanza, R. Figueira, D. C. Blanchard, and S. Parmigiani. Defensive behaviors in wild and laboratory (swiss) mice: the mouse defense test battery. *Physiol. Behav.*, 65(2):201–209, Nov. 1998.

9. O. R. Braubach, A. Fine, and R. P. Croll. Distribution and functional organization of glomeruli in the olfactory bulbs of zebrafish (danio rerio). *J. Comp. Neurol.*, 520(11):2317–39, Spc1, Aug. 2012.

10. O. R. Braubach, N. Miyasaka, T. Koide, Y. Yoshihara, R. P. Croll, and A. Fine. Experience-dependent versus experience-independent postembryonic development of distinct groups of zebrafish olfactory glomeruli. *J. Neurosci.*, 33(16):6905–6916, Apr. 2013.

11. S. A. Budick and D. M. O'Malley. Locomotor repertoire of the larval zebrafish: swimming, turning and prey capture. *J. Exp. Biol.*, 203(Pt 17):2565–2579, Sept. 2000.

12. N. S. Burghardt and E. P. Bauer. Acute and chronic effects of selective serotonin reuptake inhibitor treatment on fear conditioning: Implications for underlying fear circuits, 2013.

13. N. D. Carreau-Green, R. S. Mirza, M. L. MartÍnez, and G. G. Pyle. The ontogeny of chemically mediated antipredator responses of fathead minnowspimephales promelas, 2008.

14. X. Chen, Y. Mu, Y. Hu, A. T. Kuan, M. Nikitchenko, O. Randlett, A. B. Chen, J. P. Gavornik, H. Sompolinsky, F. Engert, and M. B. Ahrens. Brain-wide organization of neuronal activity and convergent sensorimotor transformations in larval zebrafish. *Neuron*, 100(4):876–890.e5, Nov. 2018.

15. J. S. M. Chia, E. S. Wall, C. L. Wee, T. A. J. Rowland, R.-K. Cheng, K. Cheow, K. Guillemin, and S. Jesuthasan. Bacteria evoke alarm behaviour in zebrafish. *Nat. Commun.*, 10(1):3831, Aug. 2019.

16. D. P. Chivers and R. J. F. Smith. Chemical alarm signalling in aquatic predator-prey systems: A review and prospectus, 1998.

17. M. Davis, D. L. Walker, L. Miles, and C. Grillon. Phasic vs sustained fear in rats and humans: role of the extended amygdala in fear vs anxiety. *Neuropsychopharmacology*, 35(1):105–135, Jan. 2010.

18. D. Derjean, A. Moussaddy, E. Atallah, M. St-Pierre, F. Auclair, S. Chang, X. Ren, B. Zielinski, and R. Dubuc. A novel neural substrate for the transformation of olfactory inputs into motor output. *PLoS Biol.*, 8(12):e1000567, Dec. 2010.

19. C. Diaz-Verdugo, G. J. Sun, C. H. Fawcett, P. Zhu, and M. C. Fishman. Mating suppresses alarm response in zebrafish. *Curr. Biol.*, 29(15):2541–2546.e3, Aug. 2019.

20. A. Donizetti, M. Grossi, P. Pariante, E. D'Aniello, G. Izzo, S. Minucci, and F. Aniello. Two neuron clusters in the stem of postembryonic zebrafish brain specifically express relaxin-3 gene: first evidence of nucleus incertus in fish. *Dev. Dyn.*, 237(12):3864–3869, Dec. 2008.

21. Døving B K And Kasumyan A O. Chemoreception. In *Fish Larval Physiology*. CRC Press, Jan. 2008.

22. H. Eachus, C. Bright, V. T. Cunliffe, M. Placzek, J. D. Wood, and P. J. Watt. Disrupted-in-Schizophrenia-1 is essential for normal hypothalamic-pituitary-interrenal (HPI) axis function. *Hum. Mol. Genet.*, 26(11):1992–2005, June 2017.

23. M. S. Fanselow, J. P. Decola, B. M. De Oca, and J. Landeira-Fernandez. Ventral and dorsolateral regions of the midbrain periaqueductal gray (PAG) control different stages of defensive behavior: Dorsolateral PAG lesions enhance the defensive freezing produced by massed and immediate shock, 1995.

24. R. W. Friedrich, G. A. Jacobson, and P. Zhu. Circuit neuroscience in zebrafish. *Curr. Biol.*, 20(8):R371–81, Apr. 2010.

25. K. V. Frisch. Zur psychologie des Fisch-Schwarmes, 1938.

26. T. F. Giustino and S. Maren. Noradrenergic modulation of fear conditioning and extinction. *Front. Behav. Neurosci.*, 12:43, Mar. 2018.

27. D. W. Grupe and J. B. Nitschke. Uncertainty and anticipation in anxiety: an integrated neurobiological and psychological perspective. *Nat. Rev. Neurosci.*, 14(7):488–501, July 2013.

28. S. J. Jesuthasan and A. S. Mathuru. The alarm response in zebrafish: innate fear in a vertebrate genetic model. *J. Neurogenet.*, 22(3):211–228, 2008.

29. M. Kunst, E. Laurell, N. Mokayes, A. Kramer, F. Kubo, A. M. Fernandes, D. Förster, M. Dal Maschio, and H. Baier. A Cellular-Resolution atlas of the larval zebrafish brain. *Neuron*, 103(1):21–38.e5, July 2019.

30. J. E. LeDoux, J. Iwata, P. Cicchetti, and D. J. Reis. Different projections of the central amygdaloid nucleus mediate autonomic and behavioral correlates of conditioned fear. *J. Neurosci.*, 8(7):2517–2529, July 1988.

31. H. Li, D. Pullmann, and T. C. Jhou. Valence-encoding in the lateral habenula arises from the entopeduncular region. *Elife*, 8, Mar. 2019.

32. M. Lima-Maximino, M. P. Pyterson, R. X. do Carmo Silva, G. C. V. Gomes, S. P. Rocha, A. M. Herculano, D. B. Rosemberg, and C. Maximino. Phasic and tonic serotonin modulate alarm reactions and post-exposure behavior in zebrafish. 2019.

33. Q. Lin and S. Jesuthasan. Masking of a circadian behavior in larval zebrafish involves the thalamo-habenula pathway, 2017.

34. Y.-C. Liu, I. Bailey, and M. E. Hale. Alternative startle motor patterns and behaviors in the larval zebrafish (danio rerio). *J. Comp. Physiol. A Neuroethol. Sens. Neural Behav. Physiol.*, 198(1):11–24, Jan. 2012.

35. T. Lucon-Xiccato, G. D. Mauro], A. Bisazza, and C. Bertolucci. Alarm cue-mediated response and learning in zebrafish larvae. *Behavioural Brain Research*, 380:112446, 2020.

36. A. S. Mathuru. Conspecific injury raises an alarm in medaka. *Sci. Rep.*, 6:36615, Nov. 2016.

37. A. S. Mathuru, C. Kibat, W. F. Cheong, G. Shui, M. R. Wenk, R. W. Friedrich, and S. Jesuthasan. Chondroitin fragments are odorants that trigger fear behavior in fish. *Curr. Biol.*, 22(6):538–544, Mar. 2012.

38. C. Maximino, M. G. Lima, C. C. Costa, I. M. L. Guedes, and A. M. Herculano. Fluoxetine and WAY 100,635 dissociate increases in scototaxis and analgesia induced by conspecific alarm substance in zebrafish (danio rerio hamilton 1822). *Pharmacol. Biochem. Behav.*, 124:425–433, Sept. 2014.

39. N. Miyasaka, I. Arganda-Carreras, N. Wakisaka, M. Masuda, U. Sümbül, H. S. Seung, and Y. Yoshihara. Olfactory projectome in the zebrafish forebrain revealed by genetic single-neuron labelling. *Nat. Commun.*, 5:3639, Apr. 2014.

40. U. K. Müller and J. L. van Leeuwen. Swimming of larval zebrafish: ontogeny of body waves and implications for locomotory development. *J. Exp. Biol.*, 207(Pt 5):853–868, Feb. 2004.

41. A. Nair, C. Nguyen, and M. J. McHenry. A faster escape does not enhance survival in zebrafish larvae. *Proc. Biol. Sci.*, 284(1852), Apr. 2017.

42. L. A. O'Connell and H. A. Hofmann. The vertebrate mesolimbic reward system and social behavior network: A comparative synthesis. *Journal of Comparative Neurology*, 519(18):3599–3639, 2011.

43. S. Ogawa, F. M. Nathan, and I. S. Parhar. Habenular kisspeptin modulates fear in the zebrafish. *Proc. Natl. Acad. Sci. U. S. A.*, 111(10):3841–3846, Mar. 2014.

44. S. Pandey, K. Shekhar, A. Regev, and A. F. Schier. Comprehensive identification and spatial mapping of habenular neuronal types using Single-Cell RNA-Seq. *Curr. Biol.*, 28(7):1052–1065.e7, Apr. 2018.

45. J. Panksepp, T. Fuchs, and P. Iacobucci. The basic neuroscience of emotional experiences in mammals: The case of subcortical FEAR circuitry and implications for clinical anxiety, 2011.

46. D. Ryczko and R. Dubuc. Dopamine and the brainstem locomotor networks: From lamprey to human. *Front. Neurosci.*, 11:295, May 2017.

47. B. A. Silva, C. T. Gross, and J. Gräff. The neural circuits of innate fear: detection, integration, action, and memorization. *Learn. Mem.*, 23(10):544–555, Oct. 2016.

48. R. J. F. Smith. Alarm signals in fishes, 1992.

49. M. T. Stamps, S. Go, and A. S. Mathuru. Computational geometric tools for quantitative comparison of locomotory behavior. *Sci. Rep.*, 9(1):16585, Nov. 2019.

50. P. J. Steenbergen, M. K. Richardson, and D. L. Champagne. Patterns of avoidance behaviours in the light/dark preference test in young juvenile zebrafish: a pharmacological study. *Behav. Brain Res.*, 222(1):15–25, Sept. 2011.

51. K. J. Turner, T. A. Hawkins, J. Yáñez, R. Anadón, S. W. Wilson, and M. Folgueira. Afferent connectivity of the zebrafish habenulae. *Front. Neural Circuits*, 10:30, Apr. 2016.

52. C. J. Voesenek, R. P. M. Pieters, F. T. Muijres, and J. L. van Leeuwen. Reorientation and propulsion in fast-starting zebrafish larvae: an inverse dynamics analysis. *J. Exp. Biol.*, 222(Pt 14), July 2019.

53. B. Waldman. Quantitative and developmental analyses of the alarm reaction in the zebra danio, brachydanio rerio, 1982.

54. M. F. Wullimann and K. E. Umeasalugo. Sonic hedgehog expression in zebrafish forebrain identifies the teleostean pallidal signaling center and shows preglomerular complex and posterior tubercular dopamine cells to arise from shh cells. *J. Comp. Neurol.*, Nov. 2019.

55. E. Yaksi, F. von Saint Paul, J. Niessing, S. T. Bundschuh, and R. W. Friedrich. Transformation of odor representations in target areas of the olfactory bulb. *Nat. Neurosci.*, 12(4):474–482, Apr. 2009.

56. M. D. Young and L. Lee. Fear and anxiety: Possible roles of the amygdala and bed nucleus of the stria terminalis, 1998.